



Biodistribution and Radiation Dosimetry of the Integrin Marker ^{64}Cu -BaBaSar-RGD₂ Determined from Whole-Body PET/CT in a Non-human Primate

Shuanglong Liu*, Ivetta Vorobyova, Ryan Park and Peter S. Conti

Molecular Imaging Center, Department of Radiology, Keck School of Medicine, University of Southern California, Los Angeles, CA, United States

OPEN ACCESS

Edited by:

Zhen Cheng,
Stanford University, United States

Reviewed by:

Hariprasad Gali,
University of Oklahoma Health
Sciences Center, United States
David B. Stout,
Retired, Calver City, CA, United States

Yubin Miao,
University of Colorado Denver,
United States

*Correspondence:

Shuanglong Liu
shuangll@usc.edu

Specialty section:

This article was submitted to
Biomedical Physics,
a section of the journal
Frontiers in Physics

Received: 23 August 2017

Accepted: 10 October 2017

Published: 26 October 2017

Citation:

Liu S, Vorobyova I, Park R and
Conti PS (2017) Biodistribution and
Radiation Dosimetry of the Integrin
Marker ^{64}Cu -BaBaSar-RGD₂
Determined from Whole-Body PET/CT
in a Non-human Primate.
Front. Phys. 5:54.
doi: 10.3389/fphy.2017.00054

Introduction: ^{64}Cu -BaBaSar-RGD₂ is a positron emission radiotracer taken up by integrin $\alpha_v\beta_3$, which is overexpressed in many malignancies. The aim of this study was to evaluate the biodistribution of ^{64}Cu -BaBaSar-RGD₂ in a non-human primate with positron emission tomography (PET) and to estimate the absorbed doses in major organs for human.

Materials and Methods: Whole-body PET imaging was done on a Siemens Biograph scanner with a male macaque monkey. After an i.v. injection of 13.1–19.7 MBq/kg of ^{64}Cu -BaBaSar-RGD₂, whole body scan was collected for a total duration of 180 min. Attenuation and scatter corrections were applied to reconstructions of the whole-body emission scan. After image reconstruction, three-dimensional volumes of interest (VOI) were hand-drawn on the PET transaxial or coronal slices of the frame where the organ was most conspicuous. Time-activity curves (TACs) for each VOI were obtained, and residence times of each organ were calculated by integration of the time-activity curves. Human absorbed doses were estimated using the standard human model in OLINDA/EXM software.

Results: Injection of ^{64}Cu -BaBaSar-RGD₂ was well-tolerated in the macaque monkey, with no serious tracer-related adverse events observed. ^{64}Cu -BaBaSar-RGD₂ was cleared rapidly from the blood pool, with a 12.1-min biological half-life. Increased ^{64}Cu -BaBaSar-RGD₂ uptake was observed in the kidneys, and bladder, with mean percentage injected dose (ID%) values at 1 h after injection $\sim 35.50 \pm 6.47$ and 36.89 ± 5.48 , respectively. The calculated effective dose was $15.30 \pm 2.21 \mu\text{Sv/MBq}$, and the kidneys had the highest absorbed dose at $108.43 \pm 16.41 \mu\text{Gy/MBq}$ using the non-voiding model. For an injected activity of 925 MBq ^{64}Cu for human, the effective dose would be $14.2 \pm 2.1 \text{ mSv}$.

Discussion: Due to the limited availability of the primates, we evaluated ^{64}Cu -BaBaSar-RGD₂ in the same monkey using three imaging sessions. Measured absorbed doses and

effective doses of ^{64}Cu -BaBaSar-RGD₂ are comparable to other reported RGD-derived radiopharmaceuticals labeled with ^{64}Cu and ^{18}F . Therefore, ^{64}Cu -BaBaSar-RGD₂ can be safely injected into humans for studying integrin $\alpha_v\beta_3$ expression non-invasively.

Keywords: Integrin $\alpha_v\beta_3$, ^{64}Cu -BaBaSar-RGD₂, radiation dosimetry, PET CT, non-human primate

INTRODUCTION

Tumor-induced angiogenesis plays a critical role in tumor progression and metastasis. Without new vasculature and blood circulation, tumor stops growing at the size of 1–2 mm³ and may become necrotic or even apoptotic since diffusion is already insufficient to supply the tissue with oxygen and nutrients [1, 2]. Great efforts have been made to develop therapeutic strategies that interrupt the angiogenic process to stop the tumor growth [3]. Integrin $\alpha_v\beta_3$ is a vital component for the angiogenic process by mediating endothelial cell (EC) migration and survival during angiogenesis [4]. For neovasculature formation, ECs need to migrate into an avascular region and to extensively remodel the extracellular matrix (ECM). In this process, integrins $\alpha_v\beta_3$, an immunoglobulin superfamily molecule has proved to be one of the most important cell adhesion receptors for various ECM proteins. In normal tissues, expression of integrin $\alpha_v\beta_3$ is much lower, making integrin $\alpha_v\beta_3$ an ideal target for diagnosis and therapy in cancer study. A protocol to non-invasively quantify its expression levels will provide a method to document integrin levels, which can support the anti-integrin $\alpha_v\beta_3$ treatment for the patients, and effectively monitor treatment progress for the integrin $\alpha_v\beta_3$ -positive patients. Non-invasive detection and quantification of integrin $\alpha_v\beta_3$ is also leading to the diagnosis of many types of cancer at their earliest stages [5].

Peptides containing Arg-Glu-Asp (RGD) amino acid sequence have a high binding affinity and selectivity for integrin $\alpha_v\beta_3$ [6]. In the last two decades, a number of peptides containing RGD sequences have been developed to target tumors overexpressing $\alpha_v\beta_3$ receptors [7]. RGD peptides have been modified and radiolabeled for positron emission tomography (PET) probe development. ^{18}F -galacto-RGD is the first RGD probe tested in human subjects for detecting $\alpha_v\beta_3$ expression. With conjugation of a sugar moiety for reducing the liver uptake, ^{18}F -galacto-RGD is still specifically binding to integrin $\alpha_v\beta_3$, shows a more desirable biodistribution in humans, and provides a better visualization of $\alpha_v\beta_3$ expression in tumors with high contrast [8]. However, a major disadvantage for ^{18}F -galacto-RGD is the long and sophisticated preparation, including multiple synthetic steps that complicate routine production [9]. Due to the importance of RGD peptides, continued efforts have been made to achieve desirable PET probes for easy production, optimal pharmacokinetics, and higher tumor uptake, such as ^{18}F -AH111585 [10–12], ^{18}F -alfatide [13, 14], ^{18}F -RGD-K5 [15, 16], ^{18}F -FPPRGD₂ [17, 18], ^{18}F -fluciclatide [12, 19], and ^{68}Ga -NOTA-PRGD₂ [20].

^{64}Cu [$T_{1/2} = 12.7\text{h}$; β^+ 0.653 MeV (17.8%)] has been widely used for radiolabeling proteins, antibodies and peptides for PET probe development. The low β^+ energy of ^{64}Cu gives

a resolution down to 1 mm in PET images and is important to achieve lower radiation doses for the patients [21]. Cage-like hexaazamacrobicyclic sarcophagine chelator completely encapsulates the coordinated Cu^{2+} ions. Their complexes exhibit enhanced thermodynamic and kinetic stability to copper-binding proteins *in vivo* [22]. Starting from hexaazamacrobicyclic sarcophagine, we developed the BaBaSar chelator for conjugation with RGD peptide (BaBaSar-RGD₂). The ^{64}Cu labeling chemistry for BaBaSar-RGD₂ was achieved at room temperature to give a quantitative yield. The resulted ^{64}Cu -BaBaSar-RGD₂ probe shows great stability both *in vitro* and *in vivo*, providing high tumor uptake and low normal organ uptake in U87MG glioblastoma tumor bearing mice [23]. Due to the wide application of RGD peptide in diagnostic and therapeutic applications, a novel PET radiotracer for integrin imaging with easy availability would be of great interest to both radiochemists and physicians. To promote the clinical application of ^{64}Cu -BaBaSar-RGD₂ in human, we studied its biodistribution in a non-human primate after intravenous (i.v.) administration of ^{64}Cu -BaBaSar-RGD₂ and estimated the radiation exposure for humans.

MATERIALS AND METHODS

General

All chemicals obtained commercially were of analytic grade and used without further purification. ^{64}Cu in hydrochloric acid was obtained from Washington University at St. Louis, MO. Reversed phase extraction C₁₈ Sep-Pak cartridges (Waters, Milford, MA) were pretreated with ethanol and water before use. Analytic reversed-phase high-performance liquid chromatography (RP-HPLC) using a Phenomenex Luna column (5 μm , C₁₈, 250 \times 4.6 mm) were performed on a Dionex U3000 chromatography system with a diode array detector and radioactivity flow-count (Eckert & Ziegler, Valencia, CA). The recorded data were processed using Chromeleon version 7.20 software. The flow rate of analytical HPLC was 1.0 mL/min. The mobile phase starts from 95% solvent A [0.1% trifluoroacetic acid (TFA) in water] and 5% solvent B [0.1% TFA in acetonitrile (MeCN)]. From 2 to 32 min, the mobile phase ramped to 35% solvent A and 65% solvent B. The ultraviolet (UV) detector of HPLC was set at 254 nm. The endotoxin analysis was performed on a portable Endosafe[®]-PTS[™] system consisting of LAL reagent and endotoxin controls applied to a single use, polystyrene cartridge.

Radiopharmaceutical Preparation

Production of ^{64}Cu -BaBaSar-RGD₂ suitable for monkey injection was accomplished as previous reports [23]. The final solution was passed through a 0.22 μm sterile filter (Pall Corp.).

This pyrogen-free ^{64}Cu -BaBaSar-RGD₂ possessed an acceptable pH profile (pH 5.0–7.5).

Animal Subjects

The macaque monkey studies were approved by the University of Southern California (USC) Institutional Animal Care and Use Committee (IACUC). A single male macaque monkey was used for 3 imaging sessions. The monkey (*M. fascicularis*, 8 years old) was initially anesthetized with ketamine (10 mg/kg intramuscularly) to allow preparation and handling of the animals. The animal was intubated, and connected to anesthesia equipment, and i.v. catheters were placed into right and left cephalic veins. Anesthesia was maintained by 1–3% sevoflurane during the study, and the vital signs (heart rate, respiration, and body temperature) were closely monitored and recorded for the duration of the study. ^{64}Cu -BaBaSar-RGD₂ was administered intravenously in a 3-mL dose injected with a 10- to 15-s bolus duration.

Once in the PET facility, the animal was placed on the scanner bed in a supine position during the whole scan. The animal was covered with blankets to maintain body temperature. Two intravenous lines were inserted into both cephalic veins, for the administration of the radiotracer and fluids, and for obtaining blood samples during the study, respectively.

PET/CT Acquisition

The primate underwent PET/CT imaging (Biograph Duo LSO; Siemens) immediately after intravenous administration of 111–185 MBq (3–5 mCi) of ^{64}Cu -BaBaSar-RGD₂. Low-dose unenhanced CT (pitch, 1.0; 90–130 mAs; 130 kVp) was performed before each scan. Raw CT data were reconstructed using 5-mm slice thickness transverse, and sagittal and coronal CT images were reformatted and generated to coregister to PET, accordingly. A series of 26 whole body PET images was acquired in 2-dimensional mode for a total duration of 180 min. The monkey was placed across the gantry so that one bed position of PET could cover the whole body. A 30-min static scan was acquired 22 h post injection of ^{64}Cu -BaBaSar-RGD₂. Venous blood samples were weighed right after they were withdrawn from the monkey. Decay-corrected radioactivity for each blood sample was measured in a NaI(Tl) gamma counter.

PET Reconstruction/Image Analysis

All PET/CT images were recorded in Digital Imaging and Communications in Medicine (DICOM) format and image analysis was performed using a Medical Image Data Examiner (AMIDE 1.0.4). The 26 whole-body images were analyzed individually to obtain the time-activity curves. After careful visual inspection of the images, three dimensional volumes of interests (VOIs) of each major organ were drawn on the emission frame where the organs were most clearly seen, using CT images anatomical reference. The source organs analyzed were including lungs, brain, heart, kidneys, stomach, urinary bladder, liver, and whole body. Time-activity curves (TAC) expressed as the percentage of the injected dose (% ID) at each time point were obtained by the ratio of the VOI activity to the total administered activity of ^{64}Cu -BaBaSar-RGD₂. The resulting TACs were fitted

to exponential equations, and the curves were extrapolated to the infinity using the fitted equations.

Pharmacokinetics and Metabolic Stability in Blood

After a bolus dose of ^{64}Cu -BaBaSar-RGD₂ was administered i.v. into the monkey, 100–300 μL of blood samples were collected at 1, 3, 5, 10, 20, 30, 60, 120, and 180 min after injection. The sample weights were recorded immediately and the activity of each sample was measured by the gamma-counter (Wizard 2, PerkinElmer, Waltham, MA). The pharmacokinetic parameters were calculated using non-compartmental analysis, where half-life was determined using the trapezoidal rule.

Approximately 1 mL blood samples were collected at 30 and 60 min post injection of ^{64}Cu -BaBaSar-RGD₂. Blood samples were centrifuged at 3,000 rpm for 5 min. The supernatant was treated with 100 μL trifluoroacetic acid (TFA) and centrifuged at 3,000 rpm for 3 min. The supernatant was passed through Sep-Pak C₁₈ cartridges and the cartridge was washed with 2 mL of water and the fixed activity on C₁₈ was eluted with 2 mL of acetonitrile containing 0.1% TFA. After removal of acetonitrile under reduced pressure, the residue activity was reconstituted in 1.0 mL of water and injected onto an analytic HPLC using the same gradient program with ^{64}Cu -BaBaSar-RGD₂ standard. The eluent was collected using a fraction collector (0.5 min/fraction) and the activity of each fraction was measured by a gamma-counter.

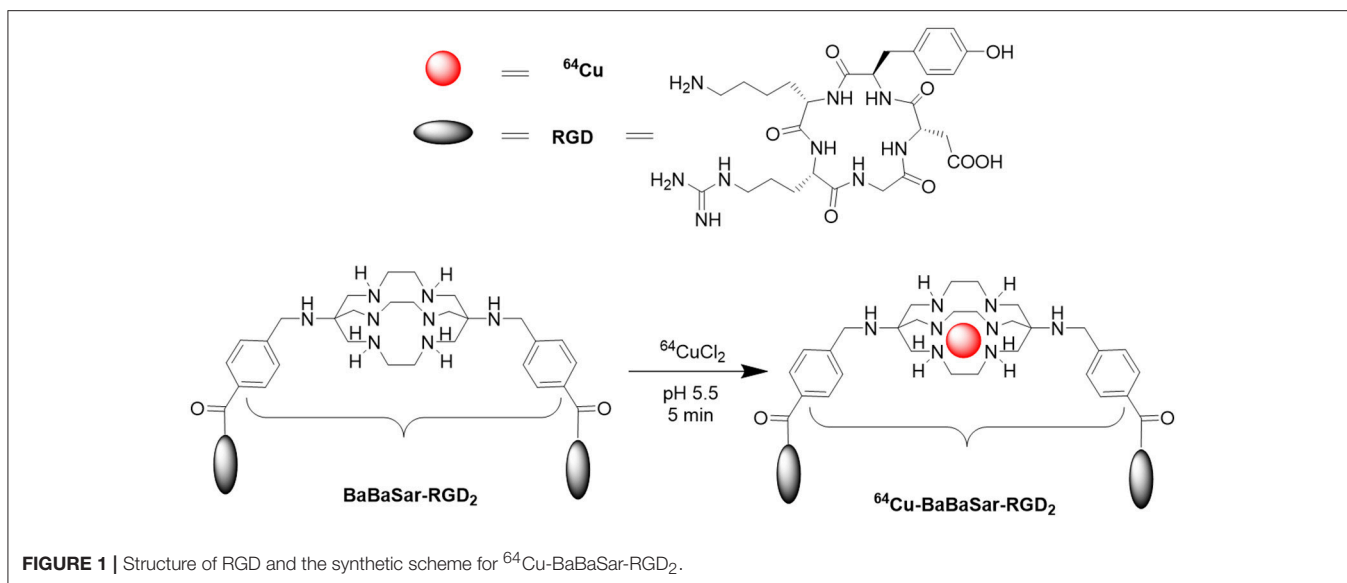
Normalized Number of Disintegrations

The %ID for each organ at all time points was fitted to an exponential or sum-of-exponentials function in OLINDA/EXM (version 1.0) software to calculate the total accumulated disintegrations per unit administered activity, which was the normalized number of disintegrations used for the dosimetry calculation. Activity in the remainder of the body at each time point was the difference between the injected activity and the activity in all the source organs. The non-voiding models for urinary bladder in OLINDA/EXM software were used to determine the normalized number of disintegrations for the bladder. Absorbed doses for each organ were calculated using the normalized number of disintegrations of all source organs for each subject. The standardized adult male and female models in OLINDA/EXM were used for the absorbed dose calculation. We assumed that the biodistribution of monkey and human are the same, therefore no adjustment of the macaque monkey biodistribution data was done for calculating human absorbed radiation doses.

RESULTS

Radiochemistry

The ^{64}Cu -labeling yield was >95%, and the radiochemical purity of ^{64}Cu -BaBaSar-RGD₂ was >99% without the need for purification (Figure 1). The retention times for free $^{64}\text{CuCl}_2$ and ^{64}Cu -BaBaSar-RGD₂ on HPLC were 2.5 and 13.9 min, respectively. The reaction crude without purifications did not show free ^{64}Cu in HPLC chromatograms. All the quality control

**TABLE 1** | Quality control data from 3 synthesis runs.

QC Test	Release criteria	Run 1	Run 2	Run 3
Product (MBq)	None	203.5	229.4	166.5
Visual inspection	Clear, colorless	Yes	Yes	Yes
Radiochemical identity	RRT = 0.9–1.1	1.0	1.0	1.0
Radiochemical purity (%)	>90	99	100	99
Specific activity (GBq/ μmol)	>3.7	15.7	14.4	22.4
Dose pH	4.5–7.5	5.5	6.0	6.0
Sterile filter integrity test (psi)	>45	64	64	62
Radionuclidic identity ($t_{1/2}$)	12.6–12.8 h	12.7	12.7	12.7
Endotoxin analysis (EU/mL)	≤ 17.5	<5	<5	<5

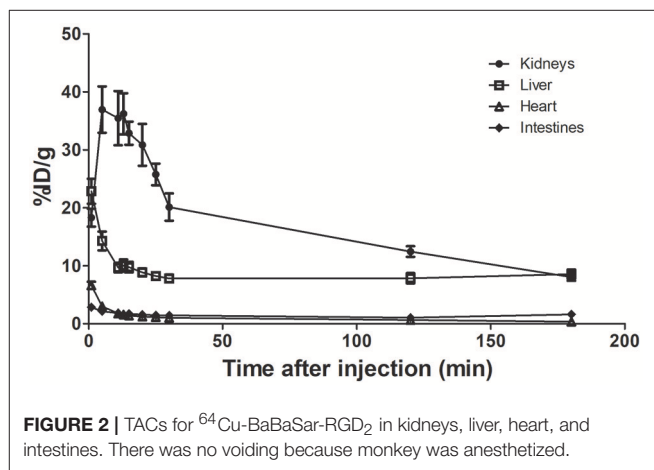
results met the pre-specified limits. These included half-life, appearance, pH value, identity, endotoxin amount, etc. (Table 1). The specific activity determined by HPLC analysis was between 14.4 and 22.4 GBq/ μmol (average 17.5 ± 4.3 GBq/ μmol). Therefore, a human dose (<925 MBq) of ^{64}Cu -BaBaSar-RGD₂ contained <125 μg of RGD peptide.

Residence-Time Calculations

Integrations of time-activity curves were used for the residence time calculation for each organ. The residence time for blood was calculated from the direct venous sample at each time point. The residence times for the spleen and red marrow were indirectly obtained from the blood samples. The spleen residence time was calculated based on its blood fraction (1.5%) of the spleen [24]. The red marrow residence time is calculated using the following equation as reported [24, 25].

$$A_{\text{rm}} = 0.19 / (1 - 0.39) A_{\text{Blood}}$$

Figure 2 shows the time-activity curve of a few major organs including kidneys, liver, heart, and intestines. Calculated from



the time-activity curves, Table 2 shows the residence times for 9 major organs.

Absorbed Dose Estimates from Macaque Imaging

The injection of 13.1–19.7 MBq/kg of ^{64}Cu -BaBaSar-RGD₂ in the macaque monkey produced no observable effects on vital signs (blood pressure, pulse, and electrocardiogram) during and 24-h after PET scan. The PET images at 1, 5, 10, 20, 40, 60, 120, and 180 min after injection are shown in Figure 3. At 1 min, rapid uptake of ^{64}Cu -BaBaSar-RGD₂ was observed in the heart, and liver. The bladder content was visualized at 10 min after injection and more and more activity was accumulated in urine bladder content. The bladder did not void because the macaque monkey was under anesthesia. Gallbladder uptake was not observed during the whole scan. Rapid clearance of activity in the liver was observed in the images at time points after 1 min. The urinary bladder had the highest uptake, with $51.37 \pm 8.73\%$ of injected

activity at 1 h post injection. The maximum uptake for the liver, and kidneys were $37.40 \pm 6.63\%ID$ (9 min) and $26.79 \pm 4.35\%ID$ (0.5 min) respectively. At 3 h of post injection, $8.62 \pm 1.41\%$ of injected activity was found in the gallbladder, small intestine, and upper and lower portions of the large intestine.

The mean organ doses for the male human phantom were calculated with Olinda/EXM using ^{64}Cu -BaBaSar-RGD₂ biodistribution in monkey (Table 3). The kidneys had the highest radiation-absorbed doses ($108.43 \mu\text{Gy}/\text{MBq}$), followed by the urinary bladder wall ($87.07 \mu\text{Gy}/\text{MBq}$). The mean effective dose of ^{64}Cu -BaBaSar-RGD₂ was $15.30 \pm 2.21 \mu\text{Sv}/\text{MBq}$. When 925-MBq of ^{64}Cu -BaBaSar-RGD₂ is administered into human subject, the effective dose for the non-voiding model is estimated to be 14.2 mSv, which is comparable to the estimated 6.23 mSv dose in a whole-body PET scan with 2-deoxy-2- ^{18}F fluoro-D-glucose (^{18}F -FDG) [26]. The estimated doses for the female human were higher by 18% because body and organ sizes of women are smaller than those men (data not shown).

Venous blood samples were withdrawn from monkey during the PET scan. Based on the decay corrected activity per unit of blood sample, we found that ^{64}Cu -BaBaSar-RGD₂ was cleared rapidly from the blood. By 3 h after injection, $2.88 \pm 0.88\%ID$ remained (range, 2.07–3.82%ID). At 22 h after injection, the activity in the blood decreased to $0.79 \pm 0.52\%ID$. Based on the

percentage of injected dose in blood sample, the half life of ^{64}Cu -BaBaSar-RGD₂ in the blood pool was calculated as 12.1 ± 4.0 min ($n = 3$).

Metabolite Analysis

Extraction efficiency of the blood samples for metabolite analysis was $\sim 75\%$. Due to the low radioactivity in blood samples, 30-s fractions from HPLC eluents were collected and radioactivity in

TABLE 3 | Estimated human absorbed doses of ^{64}Cu -BaBaSar-RGD₂ to normal organs using biodistribution data from macaque monkey.

Organs	Mean \pm SD ($\mu\text{Gy}/\text{MBq}$)
Adrenals	3.34 ± 0.52
Brain	1.27 ± 0.22
Breasts	1.34 ± 0.23
Gall bladder wall	3.07 ± 0.49
LLI wall	2.86 ± 0.44
Small intestine	4.53 ± 0.68
Stomach wall	2.11 ± 0.34
ULI wall	2.47 ± 0.39
Heart wall	4.39 ± 0.62
Kidneys	108.43 ± 16.41
Liver	7.54 ± 1.15
Lungs	1.67 ± 0.28
Muscle	1.88 ± 0.31
Ovaries	2.88 ± 0.44
Pancreas	2.86 ± 0.45
Red Marrow	9.29 ± 1.02
Osteogenic cells	7.01 ± 0.91
Skin	1.38 ± 0.24
Spleen	6.78 ± 0.88
Testes	2.03 ± 0.33
Thymus	1.56 ± 0.26
Thyroid	1.39 ± 0.24
Urinary bladder wall	87.07 ± 12.38
Uterus	4.16 ± 0.63
Total body	2.76 ± 0.42
Effective dose*	15.30 ± 2.21

TABLE 2 | Normalized number of disintegrations of source organs for macaque monkey injected with ^{64}Cu -BaBaSar-RGD₂.

Organs	Normalized no. of disintegrations (MBq-h/MBq administered)
Spleen	0.011 ± 0.002
Brain	0.018 ± 0.002
Intestines	0.023 ± 0.003
Heart	0.029 ± 0.004
Lung	0.055 ± 0.010
Liver	0.139 ± 0.021
Red Marrow	0.220 ± 0.022
Kidneys	0.403 ± 0.061
Bladder	0.435 ± 0.062
Remainder	0.818 ± 0.148

Data are mean \pm SD; $n = 3$.

*In unit of $\mu\text{Sv}/\text{MBq}$.

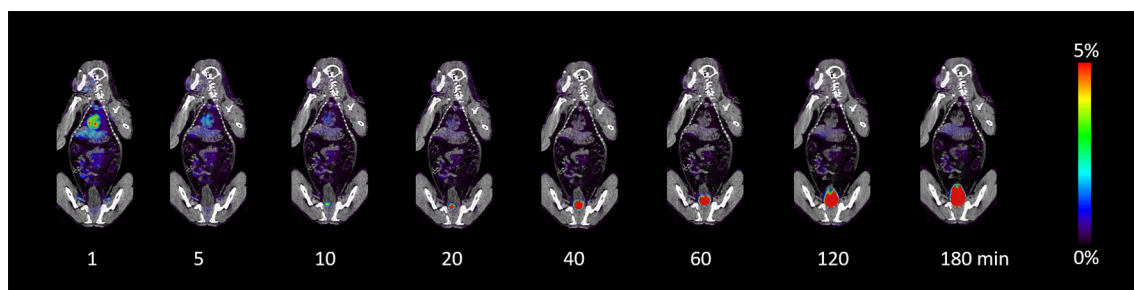


FIGURE 3 | Decay-corrected anterior maximum-intensity projections of PET/CT at 1, 5, 10, 20, 40, 60, 120, and 180 min after injection of ^{64}Cu -BaBaSar-RGD₂ in macaque monkey.

each fraction was measured using a gamma counter. Then, the radio-trace chromatograms of each blood sample were re-plotted using the activity in each fraction against the fraction time. No metabolites or free ^{64}Cu were detected by HPLC analysis of the blood samples obtained at 30 and 60 min after ^{64}Cu -BaBaSar-RGD₂ administration (**Figure 4**).

DISCUSSION

The aims of this work were to estimate the human absorbed dose in a non-human primate model before clinical use of ^{64}Cu -BaBaSar-RGD₂ for integrin $\alpha_v\beta_3$ studies. Non human primates are genetically closer to humans than any other animals, so they are considered to be the optimal substitution to study radiopharmaceuticals for human use. The results from this study demonstrate that ^{64}Cu -BaBaSar-RGD₂ is promising as a PET agent, based on the biodistribution and safety profile in monkey. With the information of the uptake levels in the monkey normal organs, the estimated radiation exposure for humans through WB PET of ^{64}Cu -BaBaSar-RGD₂ was obtained.

In the macaque monkey, the biodistribution of ^{64}Cu -BaBaSar-RGD₂ shows high uptake in the kidney and bladder and steady renal clearance. At 1 h after injection of ^{64}Cu -BaBaSar-RGD₂, 72.39 ± 10.57% of injected activity was accumulated in kidney and bladder. To our delight, ^{64}Cu -BaBaSar-RGD₂ was cleared rapidly from all the organs. The intestinal elimination of ^{64}Cu -BaBaSar-RGD₂ was indicated by gut activity loss. The liver and heart had high activity accumulation in the early stages after injection, which cleared very rapidly as time progressed.

In **Table 4**, we compared the radiation doses of ^{64}Cu -BaBaSar-RGD₂ with a few other PET probes including ^{18}F -galacto-RGD [9], ^{18}F -FDG [27], and ^{64}Cu -RGD₄ [28]. The absorbed doses in the heart, and brain were much lower for ^{64}Cu -BaBaSar-RGD₂ than those for ^{18}F -FDG. The low brain uptake could be attributed to the fact that ^{64}Cu -BaBaSar-RGD₂ could not cross the blood-brain barrier (BBB). Because the major clearance route was the urinal system, the absorbed doses of ^{64}Cu -BaBaSar-RGD₂ in urinary bladder, and kidneys were higher than those for ^{18}F -FDG. From previous reports, all the RGD-derived PET probes were excreted through the urinary system, so that the urinary bladder doses of RGD-related PET probes such as ^{18}F -Galacto-RGD, ^{64}Cu -RGD₄, and ^{64}Cu -BaBaSar-RGD₂ were much higher than that for ^{18}F -FDG. However, patients

can urinate frequently to reduce the bladder dose, which is the second highest among all the organs in this study. Comparing the dosimetry of ^{64}Cu -RGD₄ and ^{64}Cu -BaBaSar-RGD₂, we find out that ^{64}Cu -BaBaSar-RGD₂ has much higher kidney dose than ^{64}Cu -RGD₄. BaBaSar bifunctional chelator is a polyamine macrobicyclic ligand, which is more positively charged than the DOTA (tetraazacyclododecane-1,4,7,10-tetraacetic acid) counterpart in ^{64}Cu -RGD₄. The electrostatic interaction between more positively charged ^{64}Cu -BaBaSar-RGD₂ and negatively charged surface of renal proximal tubular epithelial cells would favor the re-absorption of the filtered ^{64}Cu -BaBaSar-RGD₂ by the glomerular apparatus. This re-absorption process possibly increases the retention of ^{64}Cu -BaBaSar-RGD₂ in kidneys and their corresponding radiation dose. This result is consistent with previous study for the molecular charges on the renal uptake of ^{111}In -labeled octreotide [29]. On the contrary, the liver and pancreas doses of ^{64}Cu -RGD₄ are much higher than

TABLE 4 | Organ doses in $\mu\text{Gy}/\text{MBq}$ for several pet imaging agents.

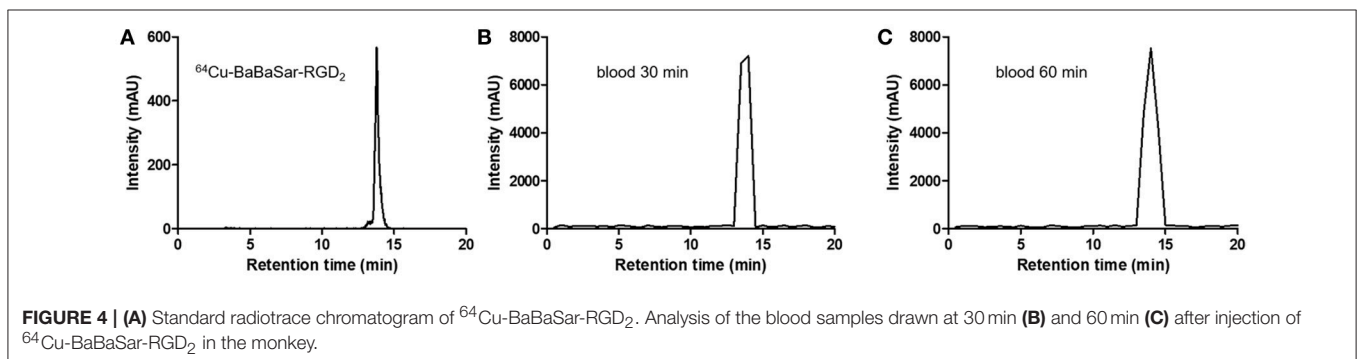
Organs	^{18}F -FDG	^{18}F -Galacto-RGD	^{64}Cu -RGD ₄	^{64}Cu -BaBaSar-RGD ₂
Adrenals	5	8.87	2.07	3.34
Brain	15.9	0.129	0.473	1.27
Breasts	3.6	0.805	0.658	1.34
GBW ¹	5.4	22.1	3	3.07
Heart wall	29	2.11	3.22	4.39
Kidneys	4.4	20.4	29.6	108.43
Liver	8.9	10.3	24.3	7.54
SI ²	5.1	219	2.19	4.53
Lungs	8.3	1.69	0.957	1.67
Muscle	4.2	6.4	1.55	1.88
Pancreas	5.2	8.34	11.5	2.86
Red marrow	4.1	8.79	1.28	9.29
Spleen	5.2	6.92	8.16	6.78
UBW ³	59.1	150	262	87.07
Total body	–	9.09	2.35	2.76
Effective dose*	8.1	37.8	16.4	15.3

*In unit of $\mu\text{Sv}/\text{MBq}$.

¹GBW, Gall bladder Wall.

²SI, Small Intestine.

³UBW, Urinary Bladder Wall.



those of ^{64}Cu -BaBaSar-RGD₂, which might be due to the higher lipophilicity of the RGD tetramer than the RGD dimer [28].

Between the monkey and human, there were many similarities on biodistribution and dosimetry data. Despite being similar physiology to humans, human effective dose using monkey data could be either underestimated or overestimated. For example, the effective dose of hypoxia marker ^{18}F -HX4 estimated from monkey study is significantly higher (42 $\mu\text{Sv}/\text{MBq}$) than the results obtained from humans (27 $\mu\text{Sv}/\text{MBq}$) [30]. Moreover, although we do not expect that the anesthesia affects the biodistribution and metabolism of ^{64}Cu -BaBaSar-RGD₂, it has been found that different anesthetic protocols can result a significant effect on the uptake of many organs [31]. Another issue to be discussed in this study is that we used a single monkey for 3 imaging sessions due to the limitation of monkey number. To make up for the limited number of animals, we performed the following arrangements. (1) The 3 imaging sessions were acquired over 8-month period. It was considerably long interval for the monkey to recover. Over this period, the monkey body weights were changed which would have an impact on the biodistribution of the tracer for statistical purpose. (2) We injected different amounts of tracer (13.1–19.7 MBq/kg) into the animal to test the variations of each scan. Our plan is to test ^{64}Cu -BaBaSar-RGD₂ in healthy volunteers and patients for integrin quantification. One injection per human will be applied in the study. The human radiation dose will be calculated and compared with this study after the first human trial with ^{64}Cu -BaBaSar-RGD₂.

REFERENCES

- Holmgren L, O'Reilly MS, Folkman J. Dormancy of micrometastases: balanced proliferation and apoptosis in the presence of angiogenesis suppression. *Nat Med.* (1995) 1:149–53.
- Parangi S, O'Reilly M, Christofori G, Holmgren L, Grosfeld J, Folkman J, et al. Antiangiogenic therapy of transgenic mice impairs *de novo* tumor growth. *Proc Natl Acad Sci USA.* (1996) 93:2002–7.
- Brown AP, Citrin DE, Camphausen KA. Clinical biomarkers of angiogenesis inhibition. *Cancer Metastasis Rev.* (2008) 27:415–34. doi: 10.1007/s10555-008-9143-x
- Brooks PC, Montgomery AM, Rosenfeld M, Reisfeld RA, Hu T, Klier G, et al. Integrin $\alpha_v\beta_3$ antagonists promote tumor regression by inducing apoptosis of angiogenic blood vessels. *Cell* (1994) 79:1157–64.
- Marelli UK, Rechenmacher F, Sobahi TR, Mas-Moruno C, Kessler H. Tumor targeting via integrin ligands. *Front Oncol.* (2013) 3:222. doi: 10.3389/fonc.2013.00222
- Plow EF, Haas TA, Zhang L, Loftus J, Smith JW. Ligand binding to integrins. *J Biol Chem.* (2000) 275:21785–8. doi: 10.1074/jbc.R000003200
- Liu S. Radiolabeled cyclic RGD peptide bioconjugates as radiotracers targeting multiple integrins. *Bioconjug Chem.* (2015) 26:1413–38. doi: 10.1021/acs.bioconjchem.5b00327
- Beer AJ, Haubner R, Wolf I, Goebel M, Luderschmidt S, Niemeyer M, et al. PET-based human dosimetry of ^{18}F -galacto-RGD, a new radiotracer for imaging $\alpha_v\beta_3$ expression. *J Nucl Med.* (2006) 47:763–9.
- Haubner R, Kuhnast B, Mang C, Weber WA, Kessler H, Wester HJ, et al. [^{18}F]Galacto-RGD: synthesis, radiolabeling, metabolic stability, and radiation dose estimates. *Bioconjug Chem.* (2004) 15:61–9. doi: 10.1021/bc034170n
- Morrison MS, Ricketts SA, Barnett J, Cuthbertson A, Tessier J, Wedge SR. Use of a novel Arg-Gly-Asp radioligand, ^{18}F -AH111585, to determine

CONCLUSION

We have successfully estimated human radiation dosimetry of ^{64}Cu -BaBaSar-RGD₂ after intravenous administration in a macaque monkey, by PET imaging and OLINDA/EXM calculations. The critical organs were kidneys and urinary bladder wall. The mean effective dose, determined with the male adult model, was $15.30 \pm 2.21 \mu\text{Sv}/\text{MBq}$. This novel PET probe demonstrates an acceptable radiation dose comparable to other reported RGD-derived radiopharmaceuticals. The findings from this investigation show great promise of ^{64}Cu -BaBaSar-RGD₂ as an integrin marker, with a desirable biodistribution and safety characteristics in monkey. Therefore, ^{64}Cu -BaBaSar-RGD₂ can safely be used for human scans for further evaluation of its performance as an integrin-targeting probe.

AUTHOR CONTRIBUTIONS

SL designed and performed research, analyzed data and wrote the paper. IV and RP performed research and analyzed data. PC designed the research and wrote the paper.

ACKNOWLEDGMENTS

This work was supported by the Whittier Foundation and University of Southern California's Molecular Imaging Center. We thank Kristin Oleary for operating the clinic PET/CT for achieving the raw data.

changes in tumor vascularity after antitumor therapy. *J Nucl Med.* (2009) 50:116–22. doi: 10.2967/jnumed.108.056077

- McParland BJ, Miller MP, Spinks TJ, Kenny LM, Osman S, Khela MK, et al. The biodistribution and radiation dosimetry of the Arg-Gly-Asp peptide ^{18}F -AH111585 in healthy volunteers. *J Nucl Med.* (2008) 49:1664–7. doi: 10.2967/jnumed.108.052126
- Kenny LM, Coombes RC, Oulie I, Contractor KB, Miller M, Spinks TJ, et al. Phase I trial of the positron-emitting Arg-Gly-Asp (RGD) peptide radioligand ^{18}F -AH111585 in breast cancer patients. *J Nucl Med.* (2008) 49:879–86. doi: 10.2967/jnumed.107.049452
- Zhou Y, Gao S, Huang Y, Zheng J, Dong Y, Zhang B, et al. A pilot study of ^{18}F -Alfatide PET/CT imaging for detecting lymph node metastases in patients with non-small cell lung cancer. *Sci Rep.* (2017) 7:2877. doi: 10.1038/s41598-017-03296-6
- Wan W, Guo N, Pan D, Yu C, Weng Y, Luo S, et al. First experience of ^{18}F -alfatide in lung cancer patients using a new lyophilized kit for rapid radiofluorination. *J Nucl Med.* (2013) 54:691–8. doi: 10.2967/jnumed.112.113563
- Mirfeizi L, Walsh J, Kolb H, Campbell-Verduyn L, Dierckx RA, Feringa BL, et al. Synthesis of [^{18}F]RGD-K5 by catalyzed [3 + 2] cycloaddition for imaging integrin $\alpha_v\beta_3$ expression *in vivo*. *Nucl Med Biol.* (2013) 40:710–6. doi: 10.1016/j.nucmedbio.2013.04.003
- Doss M, Kolb HC, Zhang JJ, Belanger MJ, Stubbs JB, Stabin MG, et al. Biodistribution and radiation dosimetry of the integrin marker ^{18}F -RGD-K5 determined from whole-body PET/CT in monkeys and humans. *J Nucl Med.* (2012) 53:787–95. doi: 10.2967/jnumed.111.088955
- Igaru A, Mosci C, Mitra E, Zaharchuk G, Fischbein N, Harsh G, et al. Glioblastoma multiforme recurrence: an exploratory study of ^{18}F FPPRGD2 PET/CT. *Radiology* (2015) 277:497–506. doi: 10.1148/radiol.2015141550

18. Iagaru A, Mosci C, Shen B, Chin FT, Mittra E, Telli ML, et al. ^{18}F -FPPRGD₂ PET/CT: pilot phase evaluation of breast cancer patients. *Radiology* (2014) 273:549–59. doi: 10.1148/radiol.14140028
19. Mena E, Owenius R, Turkbey B, Sherry R, Bratslavsky G, MacHoll S, et al. [^{18}F]fluciclatide in the *in vivo* evaluation of human melanoma and renal tumors expressing $\alpha_v\beta_3$ and $\alpha_v\beta_5$ integrins. *Eur J Nucl Med Mol Imaging* (2014) 41:1879–88. doi: 10.1007/s00259-014-2791-x
20. Li D, Zhao X, Zhang L, Li F, Ji N, Gao Z, et al. ^{68}Ga -PRGD₂ PET/CT in the evaluation of Glioma: a prospective study. *Mol Pharm.* (2014) 11:3923–9. doi: 10.1021/mp5003224
21. Chatziioannou A, Tai YC, Doshi N, Cherry SR. Detector development for microPET II: a 1 microl resolution PET scanner for small animal imaging. *Phys Med Biol.* (2001) 46:2899–910. doi: 10.1088/0031-9155/46/11/310
22. Smith SV. Molecular imaging with copper-64. *J Inorg Biochem.* (2004) 98:1874–901. doi: 10.1016/j.jinorgbio.2004.06.009
23. Liu S, Li Z, Yap LP, Huang CW, Park R, Conti PS. Efficient preparation and biological evaluation of a novel multivalency bifunctional chelator for ^{64}Cu radiopharmaceuticals. *Chemistry* (2011) 17:10222–5. doi: 10.1002/chem.201101894
24. Anderson CJ, Dehdashti F, Cutler PD, Schwarz SW, Laforest R, Bass LA, et al. ^{64}Cu -TETA-octreotide as a PET imaging agent for patients with neuroendocrine tumors. *J Nucl Med.* (2001) 42:213–21.
25. Wessels BW, Bolch WE, Bouchet LG, Breitz HB, Denardo GL, Meredith RF, et al. Bone marrow dosimetry using blood-based models for radiolabeled antibody therapy: a multiinstitutional comparison. *J Nucl Med.* (2004) 45:1725–33.
26. Huang, B, Law MW, Khong PL. Whole-body PET/CT scanning: estimation of radiation dose and cancer risk. *Radiology* (2009) 251:166–74. doi: 10.1148/radiol.2511081300
27. Quinn B, Dauer Z, Pandit-Taskar N, Schoder H, Dauer LT. Radiation dosimetry of ^{18}F -FDG PET/CT: incorporating exam-specific parameters in dose estimates. *BMC Med. Imaging* (2016) 16:41. doi: 10.1186/s12880-016-0143-y
28. Wu Y, Zhang X, Xiong Z, Cheng Z, Fisher DR, Liu S, et al. microPET imaging of glioma integrin $\alpha_v\beta_3$ expression using ^{64}Cu -labeled tetrameric RGD peptide. *J Nucl Med.* (2005) 46:1707–18.
29. Akizawa H, Arano Y, Mifune M, Iwado A, Saito Y, Mukai T, et al. Effect of molecular charges on renal uptake of ^{111}In -DTPA-conjugated peptides. *Nucl Med Biol.* (2001) 28:761–8. doi: 10.1016/S0969-8051(01)00241-4
30. Doss M, Zhang JJ, Belanger MJ, Stubbs JB, Hostetler ED, Alpaugh K, et al. Biodistribution and radiation dosimetry of the hypoxia marker ^{18}F -HX4 in monkeys and humans determined by using whole-body PET/CT. *Nucl Med Commun.* (2010) 31:1016–24. doi: 10.1097/MNM.0b013e3283407950
31. Schaafsma IA, Pollak YW, Barthez PY. Effect of four sedative and anesthetic protocols on quantitative thyroid scintigraphy in euthyroid cats. *Am J Vet Res.* (2006) 67:1362–6. doi: 10.2460/ajvr.67.8.1362

Conflict of Interest Statement: The authors declare that the research was conducted in the absence of any commercial or financial relationships that could be construed as a potential conflict of interest.

Copyright © 2017 Liu, Vorobyova, Park and Conti. This is an open-access article distributed under the terms of the Creative Commons Attribution License (CC BY). The use, distribution or reproduction in other forums is permitted, provided the original author(s) or licensor are credited and that the original publication in this journal is cited, in accordance with accepted academic practice. No use, distribution or reproduction is permitted which does not comply with these terms.